Identification of process parameters in CDA-110 copper T-shaped tube hydroforming

Do Trong Dai, Le Thanh Dat, Dinh Van Duy, Nguyen Lan Phuong, Pham Quoc Tuan*

School of Mechanical Engineering, Hanoi University of Science and Technology, 1 Dai Co Viet, Bach Mai, Hanoi, Vietnam.

*Corresponding author: tuan.phamquoc@hust.edu.vn

Received 6 May 2025; Revised 27 Jul. 2025; Accepted 20 Sep. 2025; Published 2 Oct. 2025.

DOI: https://doi.org/10.54939/1859-1043.j.mst.106.2025.145-153

ABSTRACT

This study develops a systematic method to identify the optimal process parameters of a T-shaped tube hydroforming process. Three process parameters: (1) axial displacement, (2) pressure amplification, and (3) maximum inner pressure are examined to optimize two critical performance metrics: minimum wall thickness (STH) and branch height (Height). Finite element analyses were conducted in Abaqus/Explicit to characterize the input-output relationships. Multi-objective optimization based on the Pareto front approach is applied to identify optimal process parameters that trade-off between STH and Height. Numerical validation demonstrates the effectiveness of the presented method.

Keywords: Tube hydroforming process; Process parameter identification; Multi-objective optimization; Surrogate model; Latin Hypercube Sampling; CDA-110 copper.

1. INTRODUCTION

Hydroforming has emerged as a highly efficient manufacturing process for producing complex, lightweight structures, particularly in the automotive and aerospace industries [1, 2]. Tube hydroforming processes (THF) are strongly sensitive to the implemented process parameters such as axial displacement, pressure amplification coefficient, and internal pressure [3, 4], which have been demonstrated to significantly influence deformation and defect formation. Several studies have investigated parameter identification in THFs to optimize these factors. For instance, Manabe and Amino [3] conducted numerical and experimental studies to identify optimal internal pressure and axial feed for minimizing defects like wrinkling and bursting. More recently, Xu et al. [5] utilized machine learning to optimize parameters for aluminum alloy tubes, demonstrating the potential of data-driven approaches for parameter identification in complex hydroforming processes. Experimental trials are effective in determining the process parameters, they are often time-consuming and expensive. Numerical simulations using finite element analysis (FEA), combined with statistical design of experiments and machine learning techniques, have been increasingly utilized to reduce trial-and-error efforts and provide predictive insights [6].

Copper alloy CDA-110 is frequently adopted in hydroforming applications for its exceptional ductility, electrical conductivity, and corrosion resistance. Studies on copper tube hydroforming have highlighted its unique challenges and opportunities. Pham et al. [7] assessed the formability of C1100 pure-copper tubes using an enhanced modified maximum force criterion, revealing the importance of tailored pressure profiles to prevent thinning and ensure branch formation. Trinh et al. [8, 9] applied numerical simulations to investigate the THFs to form different shapes. Additionally, Zheng et al. [4] explored hot medium pressure forming of light materials, including copper, noting that temperature and pressure adjustments are critical for enhancing formability in copper tubes. These studies underscore the need for precise parameter control to leverage copper's properties in THF applications.

This study introduces a novel framework to determine the optimal process parameters of a THF for manufacturing a T-shaped part from CDA-110 copper tubes. A huge number of numerical

simulations of the THF are conducted to create a database that will be used to train surrogate models. Then, multi-objective optimization based on the Pareto front approach is applied to identify optimal process parameters that trade-off between the minimum wall thickness (STH) and branch height (Height). Sensitivity analysis using the One-At-a-Time finite-difference method is performed on normalized parameters to quantify the dominant influence of the process parameters on both evaluation metrics.

2. CONSTITUTIVE MODEL

The tubular material used in this study is a commercial CDA-110 copper tube with an outer diameter of 22.22 mm and a wall thickness of 1 mm. Uniaxial tensile tests were conducted following the ASTM E8 standard to characterize the hardening behavior of the tested material [7]. A linear combined Swift-Voce (LSV) hardening law is adopted to model the flow stresses observed from the tests. The formula of the LSV model is expressed as follows:

$$\text{LSV: } H(\bar{\varepsilon}) = a[C(\bar{\varepsilon} + \varepsilon_0)^n] + (1-a)[A - B\exp(-k\bar{\varepsilon})] \quad (1)$$

where C, ε_0, and n are parameters from the Swift component, A, B, and k are parameters from the Voce component, and a is a weighting factor. This hardening law was chosen due to its flexibility for capturing accurately the plastic deformation of CDA-110 copper over the wide strain ranges.

This study employs the calibrated parameters of the LSV model from reference [7] without additional recalibration, since the material tested is identical to that in the previous work. The parameters, detailed in table 1, were originally determined through an iterative process to minimize discrepancies between the simulated and experimental force-displacement curves from uniaxial tensile tests. Figure 1a depicts the calibrated hardening law until a large strain value of 0.6. Moreover, these calibrated parameters yield accurate predictions of the force-displacement response, as shown in figure 1b.

Table 1. *Identified parameters of the LSV hardening law for CDA-110 copper, referred from [7].*

a	C (MPa)	ε_0	n	A (MPa)	B (MPa)	k
0.45	647.42	0.00236	0.472	393.52	333.52	0.673

Under plastic deformation, the yield condition of a material point is expressed as follows:

$$F = \bar{\sigma}(\boldsymbol{\sigma}) - H(\bar{\varepsilon}) \leq 0 \quad (2)$$

where $\bar{\sigma}(\boldsymbol{\sigma})$ is the effective stress evaluated from a yield function, and $H(\bar{\varepsilon})$ is the reference stress calculated from the LSV hardening law. For a tubular material tested in this study, the isotropic Von Mises yield function is frequently adopted to characterize the plastic deformation.

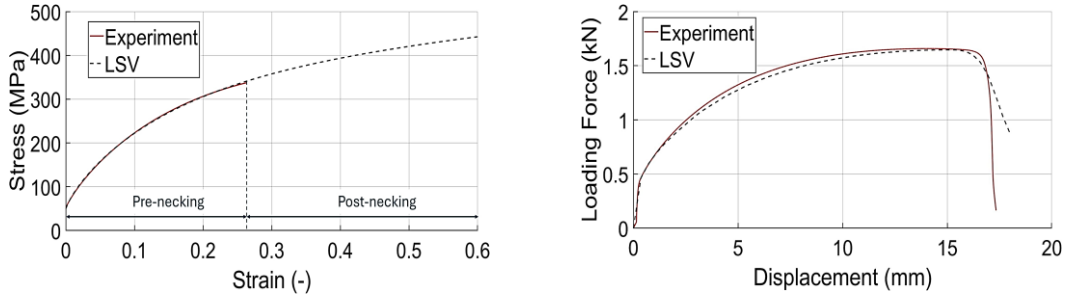

Figure 1. *Calibrated LSV hardening law for the tested material, as adopted from [7] (left) and its prediction for the force-displacement curve (right).*

3. FINITE ELEMENT ANALYSIS OF THE HYDROFORMING PROCESS

3.1. Finite element model

A finite element (FE) model is developed in Abaqus/Explicit (version 6.13) to analyze the

deformation of the copper tube subjected to a T-shaped hydroforming process. Figure 2 presents the original tube geometry with an initial length of 120mm, together with the geometry of the formed part. To reduce the computational cost, a quarter of the tube was modeled leveraging the geometric and loading symmetry of the T-shaped tube, as shown in figure 3.

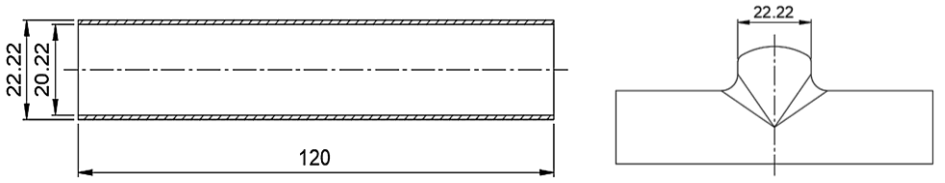

Figure 2. *Geometry of the tube before (left) and after (right) deformation.*

The tube was modeled using four-node shell elements (S4R) with the middle surface as the neutral layer. The mesh was uniformly divided into 33 elements with consistent element sizes along the tube's length and 30 elements around the circumference. The die and axial-sealing punches were modeled as perfectly rigid surfaces. Figure 3 represents an image of the die set assembly used in the numerical simulation. Consequently, symmetry boundary conditions were applied to the planes of symmetry to enforce the quarter-symmetry constraints. The free edge of the tube was subjected to an axial displacement generated by the pressor. An internal pressure was applied to the inner surface of the tube's cavity to simulate the hydraulic pressure. A friction coefficient of 0.1 was assumed to model the lubricated steel-copper contact between the tube and the die, following the recommendation in previous studies [7-9].

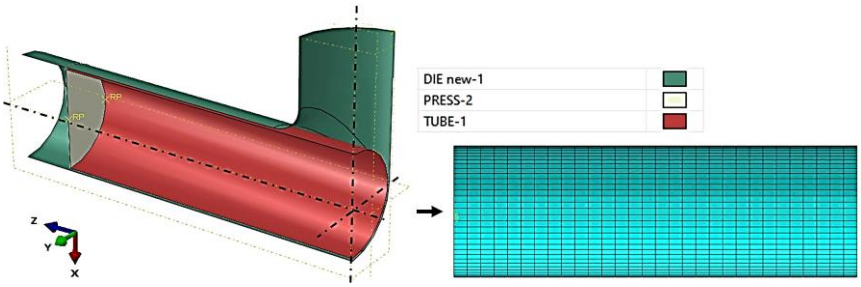

Figure 3. *Quarter-symmetry model of the T-shaped tube hydroforming process.*

Three process parameters are examined in this study due to their critical influence on the hydroforming outcome: axial displacement (X_1), pressure amplification coefficient (X_2), and the maximum internal pressure (X_3). Axial displacement (X_1, ranging from 10 to 15 mm) governs the amount of material fed into the T-branch, directly affecting the branch height and the degree of wall thinning. Higher axial displacement enhances material flow, properly increasing branch height but potentially causing excessive thinning if not balanced with other parameters [2, 3].

The pressure amplification coefficient (X_2, ranging from 0.3 to 0.9) helps to define the internal pressure increasing with respect to the simulated step time. The amplification is applied via a smooth step amplitude in Abaqus/Explicit, which uses a fifth-order polynomial to ramp the internal pressure smoothly from zero to the maximum value over the simulation time. The selected variation range of this parameter is based on preliminary simulations to ensure gradual loading to prevent abrupt stress concentrations. Moderate values of X_2 ensure stable deformation, while high values may accelerate thinning. Figure 4 presents three cases of stress amplification corresponding to different values of parameterX_2, for example, $X_2 = 0.3$, $X_2 = 0.6$, and $X_2 = 0.9$. In the first case ($X_2 = 0.3$), the pressure increases slowly during early stages of deformation, followed by a rapid rise. In contrast, the third case ($X_2 = 0.9$) exhibits a steep-pressure increase at the early stages, which subsequently slows down. Practices indicate that the selected parameter range is adequate to capture the pressure supply history observed in practical applications.

The maximum internal pressure (X_3, ranging from 40 to 60 MPa) drives the expansion of the tube into the die cavity, significantly impacting wall thickness reduction and branch formation. Higher pressures promote greater branch heights but increase the risk of thinning or rupture [5, 7]. These boundaries were calculated analytically to cover feasible loading conditions without inducing instabilities. It is worth noting that both X_2 and X_3 involve the historical development of the hydraulic pressure interacting with the tube during the deformation. Subsequently, one has to combine these two parameters to fully control the pressure history to deform the tube.

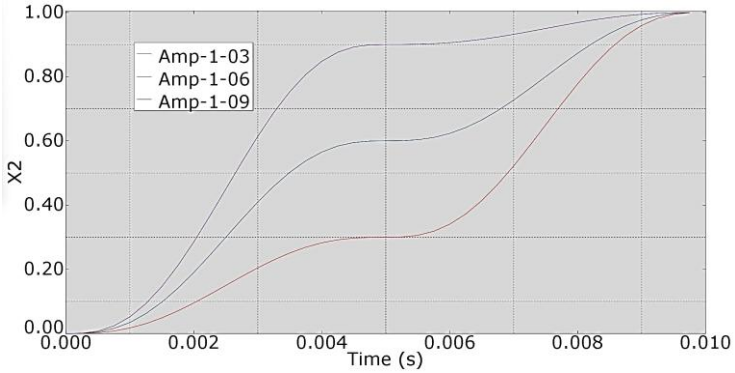

Figure 4. *Pressure amplifications examined with three values of the parameter X_2.*

Figure 5 presents simulated results obtained from a typical parameter set ($X_1 = 14.85$ mm, $X_2 = 0.812$, $X_3 = 56.05$ MPa) evaluated in Abaqus/Explicit. The simulation yields a minimum wall thickness of 0.8052 mm and a branch height of 8.716 mm. The STH typically occurs at the T-branch junction due to high tensile stresses, is a critical metric for assessing structural integrity. Maximizing STH ensures the tube can withstand operational loads without failure, such as pressure-induced rupture in fluid transport systems. Furthermore, the Height is a key geometric parameter that must be maximized to meet design specifications for applications requiring precise branch dimensions, such as piping systems. Height is determined by measuring the relative distance between the two red points, representing the branch pole and the main tube axis, as shown in the contour plot. These outputs were selected as optimization objectives to balance structural robustness with geometric accuracy.

3.2. Parameter variation

Given the computational expense of an FE simulation of THF, a sampling method is essential to efficiently explore the design space defined by the process parameters [10]. The goal is to generate a representative set of parameter combinations that capture the variability of process outcomes while minimizing the number of simulations required. This approach enables the construction of accurate surrogate models, which approximate the relationship between inputs and outputs, facilitating optimization without exhaustive simulation of all possible parameter combinations. Latin Hypercube Sampling (LHS) was selected as the sampling method due to its superior ability to provide uniform coverage of the parameter space, ensuring that each parameter range is sampled evenly and reducing the risk of clustering, which can bias surrogate model predictions [6].

The design of experiments utilized LHS to explore three process parameters (X_1, X_2, and X_3) varying within their variation ranges. A total of 50 parameter sets were generated, as visualized in figure 6, confirming even distribution across the design space. This figure illustrates a uniform distribution of samples over the design space. This visualization confirms the effectiveness of LHS in capturing the full range of each parameter without clustering, providing a robust dataset for surrogate modeling. These samples were used in the numerical simulations described in section 3.1, producing the dataset for further modeling and optimization.

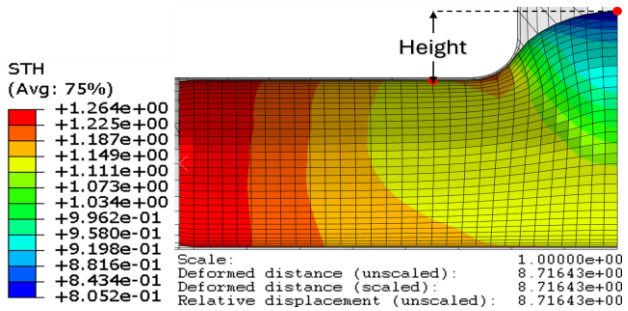

Figure 5. *Simulated results achieved with a typical parameter set.*

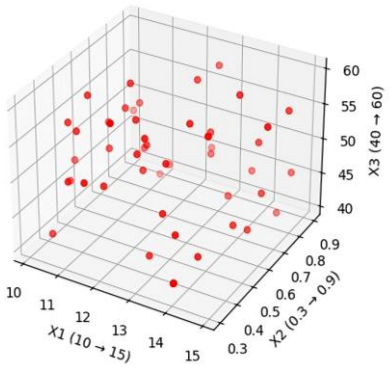

Figure 6. *Sampling 50 points with the Latin hypercube method.*

3.3. Surrogate modeling with Krigings

To facilitate multi-objective optimization of the T-shaped tube hydroforming process while addressing the computational expense of FE simulations, surrogate models were developed to predict minimum wall thickness and branch height based on three input parameters. The aim was to create efficient models that enable rapid design space exploration for NSGA-II optimization [11]. Kriging (KRG) surrogate models were selected for their ability to accurately interpolate the complex, non-linear relationships in the hydroforming process using Gaussian processes, providing robust predictions across the design space [12, 13]. The KRG models, developed in this study using the Surrogate Modeling Toolbox (SMT) [14], are available in the public repository at https://github.com/SytigamRahas/ParetoOptimization.

To ensure training stability and mitigate bias from differing scales of STH and Height, the output variables were normalized to the range [0, 1] using min-max scaling. Separate scalers were applied for STH and Height to account for their distinct physical ranges, preventing scale disparities from skewing the KRG models and enhancing numerical stability during training [14]. Two independent KRG models were trained, one for STH and another for Height, using SMT's Gaussian process framework. KRG models interpolate the data by modeling the output as a combination of a mean function and a weighted sum of Gaussian correlations, expressed as:

$$f(\mathbf{x}) = \mu + \sum_{i=1}^{n} w_i \exp\left(- \sum_{j=1}^{d} \theta_j \parallel \mathbf{x}_j - \mathbf{x}_{i,j} \parallel^2 \right) \tag{3}$$

where μ is the mean, w_i are weights, $\mathbf{x}_i$ are training points, θ_j are correlation parameters, and d is the number of input dimensions. The models were trained on the scaled dataset, with hyperparameters optimized to minimize prediction error, enabling accurate modeling of the non-linear response surfaces in hydroforming [15].

The KRG models' reliability was validated by assessing their predictive accuracy using Leave-One-Out Cross-Validation (LOOCV) error, ensuring they could generalize across the design space. The LOOCV process involved training the models on all but one data point and predicting the excluded point, repeated for each of the 50 samples, with the root mean squared error (RMSE) computed to measure performance. Figure 7 illustrates the LOOCV RMSE for both STH and Height models. The STH RMSE stabilizes around 0.0–0.1, indicating strong predictive accuracy, while the Height RMSE shows occasional spikes up to 0.8, likely due to outliers or non-linear regions in the design space. Although these spikes raise concerns about model robustness for Height, the overall low RMSE for most samples suggests acceptable generalization, with potential

improvement through outlier removal or refined hyperparameter tuning [16].

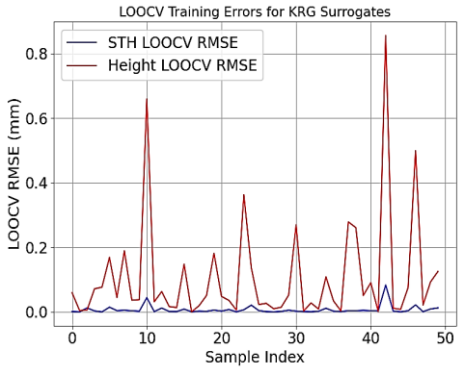

Figure 7. *LOOCV error for Kriging models of STH and height.*

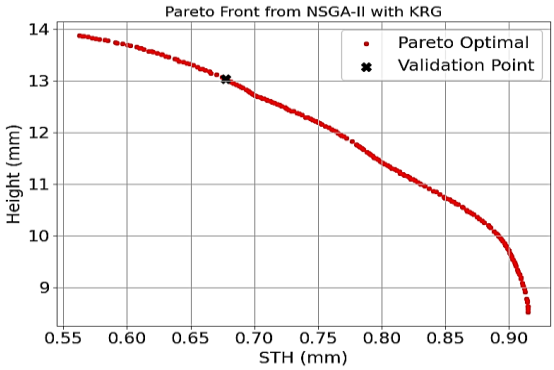

Figure 8. *Pareto-optimal solutions reflecting the trade-off between STH and height.*

4. MULTI-OBJECTIVE OPTIMIZATION

Having developed surrogate models to predict minimum wall thickness and branch height, this section focuses on optimizing the T-shaped tube hydroforming process to maximize both STH and Height. To achieve this, the NSGA-II algorithm is employed, leveraging the KRG models for efficient prediction of outcomes across the design space.

4.1. Optimization scheme

The NSGA-II algorithm, a well-established approach for multi-objective optimization, was employed via the *pymoo* library to determine optimal parameter combinations [17]. This method addresses the trade-offs between the STH and Height, guided by predictions from the KRG models, with the three process parameters serving as inputs. Since NSGA-II minimizes objectives by default, the STH and Height values were negated to achieve maximization. The algorithm used a population size of 200 and ran for 200 generations to ensure thorough exploration and convergence to a diverse solution set. Diversity was maintained with random initial sampling, Simulated Binary Crossover using a crossover distribution index $\eta_c = 15$, and Polynomial Mutation with a mutation distribution index $\eta_m = 20$.

4.2. Pareto front and optimal solutions

The optimization process yields a Pareto front, visualized in figure 8. STH values span from 0.563 to 0.915 mm, while Height ranges from 8.526 to 13.87 mm, illustrating that improving one objective often comes at the expense of the other. This trade-off is crucial for hydroforming design, as it empowers engineers to select parameters tailored to specific needs. For instance, applications demanding robust structural integrity might favor solutions with higher STH, whereas those requiring exact branch dimensions might opt for solutions with greater Height.

To validate the optimization results, a balanced solution from the Pareto front was chosen for re-simulation in Abaqus/Explicit, with parameters $X_1 = 14.94$ mm, $X_2 = 0.820$, and $X_3 = 56.80$ MPa. This point was selected because it achieves a near-maximum Height of 13.03 mm (as predicted by the KRG model) while maintaining an acceptable STH of 0.6777 mm, making it a practical compromise for applications needing both attributes. Figure 9 presents the simulated results that produce STH = 0.6710 mm and Height = 13.07 mm. Compared to the KRG predictions, the errors are 0.99% for STH and 0.31% for Height, indicating a close agreement between the surrogate model and the finite element simulation. This small discrepancy validates the KRG models' predictive accuracy and demonstrates their reliability for optimization without requiring extensive FE simulations. Such precision highlights the potential of this approach as a practical

tool for optimizing complex manufacturing processes like hydroforming.

The success of the proposed method in multi-objective optimization for parameter identification demonstrates its potential to minimize reliance on trial-and-error procedures. The use of the Pareto front map provides clear insights into trade-offs between competing objectives, enabling informed decision-making in process optimization. Furthermore, this approach can be extended to other tube hydroforming (THF) processes for manufacturing more complex geometries.

4.3. Sensitive analysis

A derivative-based global sensitivity analysis was performed to evaluate the influence of each parameter on T-tube hydroforming outcomes. For this purpose, the One-At-A-Time (OAT) finite-difference method is adopted in conjunction with the surrogate models [18, 19]. The OAT finite-difference method perturbs each parameter independently for every sample. For each of the 50 samples $\mathbf{X}^{(i)} \in \mathbb{R}^3$, the j-th parameter ($j = 1,2,3$) is adjusted by a pre-defined increment, i.e., $\Delta x_j = 0.01$. The perturbed point is then computed as:

$$\mathbf{X}^{(i)}_{\text{pert},j} = \mathbf{X}^{(i)} + \Delta x_j \mathbf{e}_j \tag{4}$$

where $\mathbf{e}_j$ is the unit vector along the j-th dimension, isolating the effect of the j-th parameter. The Kriging models predict the outputs at both the original point $f(\mathbf{X}^{(i)})$ and the perturbed point $f(\mathbf{X}^{(i)}_{\text{pert},j})$, enabling the calculation of the local sensitivity for sample i, expressed as:

$$S_j^{(i)} = \frac{|f(\mathbf{X}^{(i)}_{\text{pert},j}) - f(\mathbf{X}^{(i)})|}{\Delta x_j} \tag{5}$$

where $S_j^{(i)}$ quantifies the output change per unit perturbation, reflecting the parameter's immediate impact. The global sensitivity index for each parameter is obtained by averaging these local sensitivities across all samples, given by:

$$\bar{S}_j = \frac{1}{N}\sum_{i=1}^{N} S_j^{(i)}, \quad N = 50 \tag{6}$$

where N is the total number of samples. The global sensitivity indices $\bar{S}_j$, reported as ΔY per 1% ΔX_{scaled}, are illustrated in figure 10.

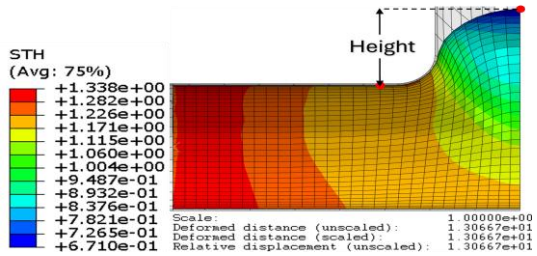

Figure 9. *Numerical validation of a representative optimal solution.*

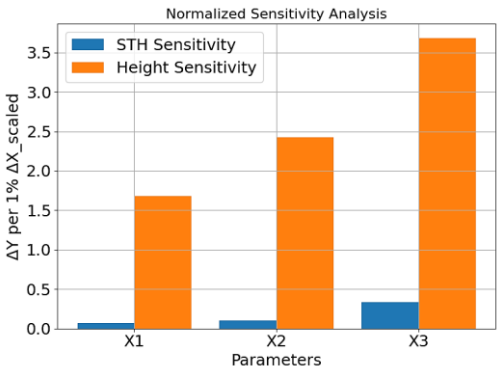

Figure 10. *Aggregated sensitivity indices for parameters X_1, X_2, and X_3 on STH and height.*

The sensitivity analysis for the STH process reveals that maximum internal pressure is the most influential parameter, with a sensitivity index of ($\bar{S}_3 = 0.33$). This indicates its dominant role in causing wall thinning through cavity expansion and material deformation. The pressure amplification

coefficient follows in significance with $\bar{S}_2 = 0.10$, while axial displacement has the least impact on thinning ($\bar{S}_1 = 0.07$). For the branch height, maximum internal pressure is once again the most critical factor, showing the highest sensitivity with $\bar{S}_3 = 3.68$. This result underscores its dominant role in driving material flow to form the branch. The other parameters show less impact with $\bar{S}_2 = 2.43$ of the pressure amplification and $\bar{S}_1 = 1.68$ of the axial displacement.

5. CONCLUSIONS

This study presents an efficient framework for optimizing the T-shaped tube hydroforming of CDA-110 copper by combining Latin Hypercube Sampling, Kriging surrogate modeling, NSGA-II optimization scheme to rapidly explore design trade-offs. This approach was successful in identifying the optimal configurations that maximize the minimum wall thickness and branch height, achieving a balance between structural integrity and geometric accuracy. Moreover, the sensitivity analysis pointed out the critical role of the maximum internal pressure in controlling wall thinning and branch formation.

A key limitation of this study is the absence of experimental validation for the predicted optimal parameters. In this regard, numerical validation presented in figure 9 verified its reliability. Future research should focus on experimental validation of optimal parameters to confirm simulated outcomes. In addition, the omission of strain rate-dependent material behavior may influence the accuracy of stress and deformation predictions under dynamic loading conditions. Incorporating a rate-dependent material model in future work could provide a more realistic representation of the hydroforming process. In particular, the influence of the X_2 parameter on pressure evolution and stress amplification is expected to become more significant when strain rate effects are considered.

REFERENCES

[1]. M. Ahmetoglu and T. Altan. *"Tube Hydroforming: State-of-the-Art and Future Trends"*, J. Mater. Process. Technol., vol. 98, no. 1, pp. 25–33, (2000).

[2]. S. Chinchanikar, H. Mulik, P. Varude, S. Atole, and N. Mundada. *"A review of emerging hydroforming technologies: design considerations, parametric studies, and recent innovations"*, J. Eng. Appl. Sci., vol. 71, no. 1, p. 205, (2024).

[3]. K. I. Manabe and M. Amino. *"Effects of process parameters and material properties on deformation process in tube hydroforming"*, J. Mater. Process. Technol., vol. 123, no. 2, pp. 285–291, (2002).

[4]. K. Zheng, J.-H. Zheng, Z. He, G. Liu, D. J. Politis, and L. Wang. *"Fundamentals, Processes and Equipment for Hot Medium Pressure Forming of Light Material Tubular Components"*, Int. J. Lightweight Mater. Manuf., vol. 3, no. 1, pp. 1–19, (2020).

[5]. Y. Xu, X. Zhang, W. Xie, S. Zhang, Y. Tian, and L. Chen. *"Optimisation of Aluminium Alloy Variable Diameter Tubes Hydroforming Process Based on Machine Learning"*, Appl. Sci., vol. 15, no. 9, p. 5045, (2025).

[6]. N. V. Queipo, R. T. Haftka, W. Shyy, T. Goel, R. Vaidyanathan, and P. K. Tucker. *"Surrogate-based analysis and optimization"*, Prog. Aerosp. Sci., vol. 41, no. 1, pp. 1–28, (2005).

[7]. N. A. Pham, Q. T. Pham, V. D. Dinh, D. T. Nguyen, D.-T. Nguyen, T. D. Hoan, L. D. Giang. *"Formability Assessment of C1100 Pure-Copper Tube Considering an Enhanced Modified Maximum Force Criterion"*, Materials, vol. 18, no. 9, p. 1919, (2025).

[8]. M. T. Trinh, T. D. Nguyen, Q. T. Pham, A. N. Pham, D. V. Dinh. *"Hydro-Forming of U-Shaped Parts with Branches"*, Engineering, Technology & Applied Science Research, vol. 15, no. 1, (2025).

[9]. M. T. Trinh, D. T. Nguyen, T. Q. Pham, A. N. Pham, V. D. Dinh. *"Hydro-Forming a Cross-Shaped Component from Tube Billet"*, Journal of Machine Engineering, vol. 25, no. 2, pp. 111–122, (2025).

[10]. D. C. Montgomery. *Design and Analysis of Experiments*, 10th ed., Hoboken, NJ, USA: Wiley, (2019).

[11]. K. Deb, A. Pratap, S. Agarwal, and T. Meyarivan. *"A Fast and Elitist Multiobjective Genetic Algorithm: NSGA-II"*, IEEE Trans. Evol. Comput., vol. 6, no. 2, pp. 182–197, (2002).

[12]. M. S. Chebbah and N. Lebaal. *"Tube hydroforming optimization using a surrogate modeling approach and Genetic Algorithm"*, Mech. Adv. Mater. Struct., vol. 27, no. 6, pp. 515–524, (2018).

[13]. Z. Zhang, F. Xu, and X. Sun. *"Optimization of process parameters during hydroforming of tank bottom using NSGA-III algorithm"*, Int. J. Adv. Manuf. Technol., vol. 119, pp. 4043–4055, (2022).
[14]. P. Saves, R. Lafage, N. Bartoli, Y. Diouane, J. H. Bussemaker, T. Lefebvre, J. T. Hwang, J. Morlier, and J. R. R. A. Martins. *"SMT 2.0: A Surrogate Modeling Toolbox with a focus on Hierarchical and Mixed Variables Gaussian Processes"*, Advances in Engineering Software, (2024).
[15]. T. Huang, X. Song, and M. Liu. *"A Kriging-based non-probability interval optimization of loading path in T-shape tube hydroforming"*, Int. J. Adv. Manuf. Technol., vol. 85, no. 5, pp. 1615–1631, (2016).
[16]. B. Phipson, S. C. Lee, I. Majewski, W. Alexander, and G. Smyth. *"Robust hyperparameter estimation protects against hypervariable genes and improves power to detect differential expression"*, Annals of Applied Statistics, vol. 10, no. 2, pp. 946–963, (2016).
[17]. J. Blank and K. Deb. *"pymoo: Multi-objective optimization in Python"*, IEEE Access, vol. 8, pp. 89497–89509, (2020).
[18]. W. Dan, X. Yue, M. Yu, T. Li, and J. Zhang. *"Prediction and Global Sensitivity Analysis of Long-Term Deflections in Reinforced Concrete Flexural Structures Using Surrogate Models"*, Materials, vol. 16, no. 13, (2023).
[19]. A. Saltelli, P. Annoni, I. Azzini, F. Campolongo, M. Ratto, and S. Tarantola. *"Variance Based Sensitivity Analysis of Model Output. Design and Estimator for the Total Sensitivity Index"*, Comput. Phys. Commun., vol. 181, no. 2, pp. 259–270, (2010).

TÓM TẮT

Tối ưu hóa thông số công nghệ cho quá trình dập thủy tĩnh phôi ống đồng CDA-110 để chế tạo chi tiết dạng chữ T

Nghiên cứu này phát triển một phương pháp có hệ thống nhằm tối ưu hóa các thông số công nghệ trong quá trình dập thủy tĩnh phôi ống đồng CDA-110 để chế tạo chi tiết dạng chữ T. Ba thông số quá trình, gồm có (1) độ dịch chuyển trục dọc trục, (2) hệ số khuếch đại áp suất và (3) áp suất tối đa, được khảo sát để tối ưu hoá đồng thời hai chỉ tiêu chất lượng quan trọng: độ dày thành tối thiểu (STH) và chiều cao nhánh (Height). Phân tích phần tử hữu hạn được thực hiện trong phần mềm Abaqus/Explicit để mô tả chi tiết mối quan hệ giữa đầu vào và đầu ra. Phương pháp tối ưu đa mục tiêu dựa trên tập hợp Pareto được áp dụng nhằm xác định bộ thông số quy trình tối ưu, đảm bảo tính cân bằng giữa STH và Height. Kết quả xác thực bằng mô phỏng số cho thấy hiệu quả và tính khả thi của phương pháp được đề xuất.

Từ khoá: Dập thuỷ tĩnh phôi ống; Xác định các thông số công nghệ; Tối ưu hoá đa mục tiêu; Mô hình thay thế; Latin hypercube sampling; Hợp kim đồng CDA-110.